This article was downloaded by:
On: *25 January 2011*
Access details: *Access Details: Free Access*
Publisher *Taylor & Francis*
Informa Ltd Registered in England and Wales Registered Number: 1072954 Registered office: Mortimer House, 37-41 Mortimer Street, London W1T 3JH, UK

Separation Science and Technology
Publication details, including instructions for authors and subscription information:
http://www.informaworld.com/smpp/title~content=t713708471

Solvent Vapor Recovery by Pressure Swing Adsorption. II. Experimental Periodic Performance of the Butane-Activated Carbon System

Yujun Liu; Charles E. Holland; James A. Ritter

To cite this Article Liu, Yujun , Holland, Charles E. and Ritter, James A.(1998) 'Solvent Vapor Recovery by Pressure Swing Adsorption. II. Experimental Periodic Performance of the Butane-Activated Carbon System', Separation Science and Technology, 33: 16, 2431 — 2463
To link to this Article: DOI: 10.1080/01496399808545313
URL: http://dx.doi.org/10.1080/01496399808545313

PLEASE SCROLL DOWN FOR ARTICLE

Full terms and conditions of use: http://www.informaworld.com/terms-and-conditions-of-access.pdf

This article may be used for research, teaching and private study purposes. Any substantial or systematic reproduction, re-distribution, re-selling, loan or sub-licensing, systematic supply or distribution in any form to anyone is expressly forbidden.

The publisher does not give any warranty express or implied or make any representation that the contents will be complete or accurate or up to date. The accuracy of any instructions, formulae and drug doses should be independently verified with primary sources. The publisher shall not be liable for any loss, actions, claims, proceedings, demand or costs or damages whatsoever or howsoever caused arising directly or indirectly in connection with or arising out of the use of this material.

SEPARATION SCIENCE AND TECHNOLOGY, 33(16), pp. 2431–2463, 1998

Solvent Vapor Recovery by Pressure Swing Adsorption. II. Experimental Periodic Performance of the Butane–Activated Carbon System

YUJUN LIU, CHARLES E. HOLLAND, and JAMES A. RITTER*
DEPARTMENT OF CHEMICAL ENGINEERING
SWEARINGEN ENGINEERING CENTER
UNIVERSITY OF SOUTH CAROLINA
COLUMBIA, SOUTH CAROLINA 29208, USA

Downloaded At: 11:17 25 January 2011

ABSTRACT

An experimental investigation was carried out for the separation and recovery of butane vapor (10 to 40 vol%) from nitrogen using Westvaco BAX activated carbon and a unique pressure swing adsorption (PSA)–solvent vapor recovery (SVR) system. The effects of six important process and operating parameters on the periodic process performance were obtained, i.e., the purge-to-feed ratio, purge pressure, volumetric feed flow rate, feed concentration, cycle time, and pressurization/blowdown step time. Overall, the experimental results were consistent with theoretical results in the literature for the effects of most of these parameters; however, some opposite and unique trends were observed. The experimental results verified that the concentration wave front may be contained within the bed even when the purge-to-feed ratio is less than unity, and that the process performance may be very sensitive to minor changes in the purge pressure. Moderate temperature swings (18 to 54°C) were exhibited in all cases, and they decreased with increasing bed coverage, especially when breakthrough occurred. Also, when the bed coverage increased, the mass transfer zone also increased. Finally, these experimental results provided significant insight into designing more efficient PSA–SVR processes and developing new PSA–SVR cycle configurations for improved solvent vapor enrichment.

* To whom correspondence should be addressed. Telephone: (803) 777-3590. FAX: (803) 777-8265. E-mail: ritter@sun.che.sc.edu

Copyright © 1998 by Marcel Dekker, Inc. www.dekker.com

INTRODUCTION

Over the past two decades, the industrial and academic focus on the development of most PSA processes has been on the purification and recovery of the light component; the heavy component was simply an undesirable vent gas. However, this focus has changed with the recent commercialization of a pressure swing adsorption (PSA) process for solvent vapor recovery (SVR) (1, 2). As a result, the understanding of PSA for heavy product enrichment and recovery is increasing, but both the theoretical and experimental studies are still in their infancy.

Ritter and Yang (3, 4) studied PSA for air purification and vapor recovery by experiment and simulation for the removal of dimethyl methylphosphomate (DMMP) vapor from air. Further modeling work was done by Kikkinides et al. for the recovery of hexane vapor (5). Modeling studies were also carried out by Kikkinides and Yang (6) to investigate a PSA process for SO_2/NO_x removal and SO_2 recovery from flue gas, by Kikkinides et al. (7) and Chue et al. (8) to investigate a PSA process for CO_2 recovery from flue gas, and by Kikkinides et al. (9) to investigate the feasibility of a PSA–natural gas desulfurization process. SO_2 recovery by PSA was investigated experimentally by Izumi et al. (10), and the recovery of CO_2 by PSA from a molten carbonate fuel cell system was studied in a test plant by Sasaki et al. (11). An unusual experimental and theoretical study was carried out by Ruthven and Farooq (12) for the separation of hydrogen/tritium from a dilute helium stream using a cryogenic vacuum swing cycle. Suh and Wankat (13) presented a theoretical analysis of a new PSA process for high enrichment and recovery of the strongly adsorbed component, which utilized an inert column between two adsorbent columns for compression and recycling of the strongly adsorbed component using the weakly adsorbed component. LeVan (14) developed a unique isothermal equilibrium theory to investigate some interesting features of the PSA–SVR system, such as the direct determination of the periodic state, the minimum bed depth required for operation at different purge-to-feed ratios, and the extent of accumulation of adsorbate in the bed for different favorable Langmuir-type isotherms. Subramanian and Ritter (15) extended this model to accommodate the case of breakthrough of the solvent vapor into the light product; they also obtained analytical expressions for the solvent vapor enrichment and recovery, and the light product impurity. Recently, the major assumptions commonly utilized in PSA–SVR process simulations were evaluated by Liu and Ritter (16). They also studied a PSA process for benzene vapor recovery by computer simulation (17), where the effects of nine process and operating parameters on the process performance were analyzed. A fractional factorial analysis was also performed on the effects of seven important parameters on the PSA–benzene vapor recovery

Downloaded At: 11:17 25 January 2011

process (18), where some interesting parameter interaction effects were revealed. Finally, using computer simulation, these authors discovered unusual periodic state heat effects that affected the performance of a PSA–butane vapor recovery process (19).

The 19 articles cited above all dealt with the heavy component enrichment and recovery. However, only five of the 19 presented any experimental results (3, 4, 10, 11, 12), and only two of these five actually dealt with a PSA–SVR process (3, 4). But these two studies were mainly concerned with air purification; the concept of heavy component enrichment and recovery was introduced simply as an interesting observation. Therefore, the objective of this study was to carry out a first-time experimental investigation of an actual PSA–SVR process at the bench-scale. *n*-Butane vapor recovery from nitrogen using BAX (Westvaco) activated carbon was chosen because of its commercial relevance. It represents one of the lighter components escaping from the liquid phase during the bulk transfer of gasoline from various storage vessels (20). In a series of experiments, transient and periodic results were obtained demonstrating the process dynamics and performance of this system. Part I (21) described the PSA system and reported unique transient and periodic dynamic behavior. In this paper (Part II), the periodic performance of the process is reported.

Downloaded At: 11:17 25 January 2011

EXPERIMENTAL

PSA Process Description

The PSA cycle utilized in this study was a Skarstrom-type cycle. During each cycle, two beds each underwent four steps, namely, (I) pressurization, (II) adsorption, (III) blowdown, and (IV) purge. While one bed was undergoing adsorption the other bed was being purged, and while one bed was undergoing repressurization the other bed was being depressurized. In this way the beds operated 180° out-of-phase with each other. Eventually, these coupled beds reached a periodic state where the time-dependent bed profiles and effluent concentration histories were reproduced from cycle to cycle. Additional details of the process were given in Part I (21).

Apparatus and Procedure

Details on the apparatus and procedure were given in Part I (21). The transient approach to the periodic state was also discussed, and the periodic behavior was verified whether starting from a completely regenerated or contaminated bed as long as the periodic state resulted in a more contaminated bed compared to the initial condition. This periodic state verification was important because of the way each series of runs was carried out.

Initially, both beds were regenerated at 135 ± 15°C for 16 hours using a nitrogen purge under vacuum. The nitrogen purge was approximately 0.125 SLPM through each bed, and the vacuum level was approximately 3 kPa. For each series of runs, corresponding to the study of a particular parameter, the PSA process was initiated with completely regenerated beds cooled to room temperature and blanketed with nitrogen. Also, for each series of runs the parameter of interest was set first at a value corresponding to the smallest bed penetration. All other process variables were fixed. Once the periodic state was reached, the value of this parameter was changed to the next value without stopping the process, and the system was allowed to reach the new periodic state. In this way a series of runs were carried out continuously, where the bed became progressively more contaminated with each run. After one series of runs was completed, the PSA process was stopped and the beds were regenerated as specified above. After the columns cooled down to the ambient temperature, the next series of runs commenced. This procedure was repeated until all of the runs were completed.

Downloaded At: 11:17 25 January 2011

Process Performance Indicators

The process performance was analyzed according to the solvent vapor enrichment (E) and recovery (R), the light product purity (y_p), and the bed capacity factor (BCF) (17). The solvent vapor enrichment was defined as the average mole fraction of the solvent vapor leaving the bed during Steps III and IV divided by the mole fraction of the solvent vapor in the feed. The solvent vapor recovery was defined as the ratio of the number of moles of the solvent vapor leaving the bed during Steps III and IV to the number of moles of the solvent vapor entering the bed during Step II. The light product purity was defined as the average mole fraction of the solvent vapor exiting the light product end during Step II. The bed capacity factor was defined as

$$\text{BCF} = \int_0^L q\, dz/q_f^* L \tag{1}$$

and represents the capacity of the bed that was used at the periodic state (measured at the end of Step II) compared to the maximum capacity of the bed at the feed conditions.

The solvent vapor enrichment was calculated using the effluent concentration histories sampled under both positive and negative gauge pressures using gas-tight syringes. Typically, nine to eleven samples were taken during each of the blowdown and purge steps. The average mole fraction of the solvent vapor during Steps III and IV was taken as the time average of the mole fraction in all of the samples taken during these two steps. The light product purity was also obtained in a similar fashion using the gas-tight syringes.

Again, nine to eleven samples were taken from the light product stream, and the light product purity was taken as the time average of the mole fraction in all of the samples collected during Step II.

The solvent vapor recovery was calculated by using the time-dependent light product mole fraction determined above, coupled with the time-dependent volumetric flow rate of the light product recorded by the mass flowmeter. The amount of butane leaving the bed during the adsorption step was calculated by integration of these quantities. This quantity, subtracted from and then divided by the amount of butane fed into the bed during the feed step, gave the solvent vapor recovery.

Since the adsorbed phase loadings were not measured directly, the bed capacity factor defined by Eq. (1) was approximated using a modified form given by

$$\text{BCF} = \int_0^L q_z^* dz / q_f^* L \tag{2}$$

The isotherm model used to calculate q_z^* was the three-process Langmuir model (TPLM) (19), represented by Eqs. (3) to (5):

$$q^* = \sum_{i=1}^{3} \frac{q_{mi} b_i P y}{1 + b_i P y}, \qquad i = 1, 2, 3 \tag{3}$$

$$q_{mi} = q_{0i} \exp\left(\frac{A_i}{T}\right) \tag{4}$$

$$b_i = b_{0i} \exp\left(\frac{B_i}{T}\right) \tag{5}$$

This TPLM was fitted simultaneously to butane–BAX activated carbon isotherms measured at 25 and 50°C (20) to determine the 12 parameters using nonlinear regression. The average relative error (ARE) defined as

$$\text{ARE} = \frac{100}{N} \sum_{i=1}^{N} \text{abs}\left(\frac{q_{\text{exp},i} - q_{\text{cal},i}}{q_{\text{exp},i}}\right)\% \tag{6}$$

was 5.3%. Figure 1 compares the model correlation (solid lines) with the experimental data (symbols). The TPLM parameters are given in Table 1. The required information for the TPLM was obtained from the bed pressure and the nine-point periodic state gas-phase concentration and temperature profiles obtained at the end of the adsorption step.

RESULTS AND DISCUSSION

A series of 24 experiments were carried out to study the periodic state recovery of butane vapor from nitrogen using BAX-activated carbon and the unique

Downloaded At: 11:17 25 January 2011

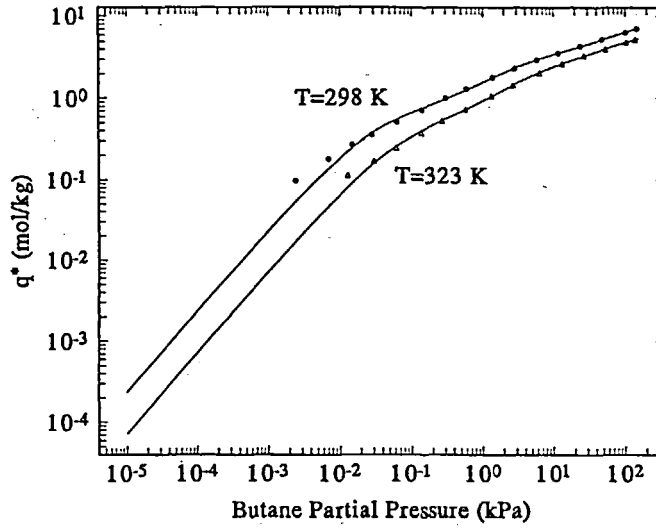

FIG. 1 Experimental equilibrium adsorption isotherms of *n*-butane vapor on BAX activated carbon at 298 K (●) and 323 K (Δ): lines represent the correlations with the three-process Langmuir model.

Downloaded At: 11:17 25 January 2011

PSA–SVR system. The effects of six important parameters on the PSA–SVR process performance were investigated. The six parameters were the volumetric purge-to-feed ratio (γ), purge pressure (P_L), volumetric feed flow rate (V_f), feed concentration (y_f), cycle time (t_c), and pressurization/blowdown step time (t_{pb}). Process conditions similar to those used commercially were chosen for each series of experiments; they are given in Table 2. The effects of these parameters on the process performance are summarized in Table 3.

During each series of runs an attempt was made to fix all of the parameters except for the one being investigated. This included the pressure histories,

TABLE 1
Three Process Langmuir Model Adsorption Isotherm Parameters[a]

	q_0 (mol/kg)	A (K)	b_0 (kPa^{-1})	B (K)
Process 1	0.004814	1497.18	0.0006985	3184.0
Process 2	0.22621	737.289	0.0002652	2205.951
Process 3	0.17997	1067.552	0.0023777	400.457

[a] See Eqs. (3) to (5).

TABLE 2
PSA–SVR Process Conditions[a] and Periodic Process Performance

Run	V_f (1 STP/min)	γ (—)	y_f (%)	t_c (min)	t_{pb} (min)	P_L (kPa)	E (—)	R (%)	BCF (—)	y_P (—)
A1	2.5	*1.41*	*21.2*	20	2	*14.7*	2.26	100	0.29	0.0
A2	2.5	*1.28*	20.8	20	2	13.5	2.55	100	0.33	0.0
A3	2.5	*1.14*	21.8	20	2	12.2	2.72	100	0.36	0.0
A4	2.5	*0.50*	20.4	20	2	13.7	3.62	100	0.44	0.0
A5	2.5	*0.24*	20.8	20	2	14.6	4.22	85.9	0.81	3.4×10^{-2}
B1	2.5	1.45	19.9	20	2	*28.3*	1.80	100	0.30	0.0
B2	2.5	1.49	20.3	20	2	*41.4*	1.55	100	0.31	0.0
B3	2.5	1.48	19.6	20	2	*55.7*	1.46	100	0.35	0.0
B4	2.5	1.50	20.4	20	2	*68.8*	1.40	100	0.38	0.0
C1	*1.5*	1.48	19.7	20	2	13.9	2.01	100	0.17	0.0
C2	*2.5*	1.50	20.9	20	2	13.8	2.32	100	0.30	0.0
C3	*3.5*	0.86	20.6	20	2	23.9	2.95	97.2	0.74	6.7×10^{-3}
C4	*4.0*	0.80	20.6	20	2	26.5	3.12	91.9	0.83	1.9×10^{-2}
D1	2.5	1.41	*9.5*	20	2	14.6	3.30	100	0.22	0.0
D2	2.5	1.17	*31.4*	20	2	17.6	1.67	100	0.38	0.0
D3	2.5	0.94	*39.3*	20	2	22.0	1.54	100	0.62	0.0
E1	2.5	0.74	34.0	*10*	1.0	27.7	1.42	100	0.32	0.0
E2	2.5	0.73	34.9	*15*	1.5	28.3	1.71	100	0.47	0.0
E3	2.5	0.69	35.8	*20*	*2.0*	29.8	2.01	99.0	0.73	5.8×10^{-3}
E4	2.5	0.73	35.3	*25*	2.5	28.4	1.96	97.8	0.81	1.3×10^{-2}
E5	2.5	0.76	35.6	*30*	3.0	26.9	1.95	92.4	0.82	4.4×10^{-2}
F1	2.5	0.76	34.5	26	*5*	27.2	2.04	99.4	0.67	3.6×10^{-3}
F2	2.5	0.75	34.9	24	*4*	27.3	2.06	99.3	0.71	4.2×10^{-3}
F3	2.5	0.74	34.4	22	*3*	27.8	2.00	99.0	0.73	5.6×10^{-3}

[a] The adsorption (Step II) pressure for all runs was approximately 151.6 kPa.

TABLE 3
PSA–SVR Periodic Process Performance Summary

Parameter	Effects on the PSA–SVR process performance			
	R	E	y_p	BCF
↑γ	↑	↓	↓	↓
↑V_f	↓	↑	↑	↑
↑y_f	100%	↓	0.0	↑
↑t_c	↓	↑↓	↑	↑
↑t_{pb}[a]	↓	↑	↑	↑
↑P_L	100%	↓	0.0	↑

[a] The effect of t_{pb} on all of the process performance indicators was almost negligible.

Downloaded At: 11:17 25 January 2011

where in each run the pressurization rate was adjusted so that the feed pressure was reached by the end of Step I; and an attempt was made to also control the blowdown rate so that the purge pressure was reached by the end of Step III. In this way the pressure histories associated with each series of runs were forced to exhibit similar trends. The six sets of periodic state pressure histories are displayed in Fig. 2. Notable differences are apparent, but only in Figures 2(B), 2(C), and 2(D), the other three cases exhibited similar trends. The effects of these differences are discussed below in the respective sections.

Effect of the Purge-to-Feed Ratio

In PSA systems the purge-to-feed ratio is always selected as one of the most important design variables as it controls not only the purity and recovery of the light component but also the enrichment of the heavy component (3, 4, 17). Therefore, five experiments were performed to investigate the effect of the volumetric purge-to-feed ratio (Runs A1 to A5 in Table 2). The purge-to-feed ratio was defined as the ratio of the purge gas velocity at the purge pressure (P_L) to the feed gas velocity at the adsorption or feed pressure (P_H), since the adsorption and purge step times were equal (17). The magnitude of the volumetric purge-to-feed ratio was varied from 1.41 to 0.24 by decreasing the purge flow rate. All of the other conditions were fixed (see Table 2), including the pressure histories.

Figure 2(A) displays the pressure histories for four of these five runs during a periodic cycle. The pressure histories for all of these runs were remarkably quite consistent. This result assured that the effects discussed below were most likely caused by a change in the purge-to-feed ratio and not by a change in some other process variable.

The butane vapor concentration and temperature profiles at the beginning and end of the adsorption step for some of these runs are shown in Fig. 3. At the end of the adsorption step, as the purge-to-feed ratio decreased, the concentration wave front moved toward the light product end of the bed, with a corresponding increase in the mass transfer zone (MTZ) and a decrease in the peak bed temperature. The peak temperature in the bed was approximately 57°C and occurred with the largest purge-to-feed ratio. At the beginning of the adsorption step, as the purge-to-feed ratio decreased, less of the concentration wave front was pushed out of the bed, giving rise to smaller concentration swings over a cycle, especially for the purge-to-feed ratio of 0.24. Also, the temperatures within the MTZ were always below the ambient (or feed) temperature, with the lowest temperature reaching approximately 13°C. But the effect of the purge-to-feed ratio on these temperatures at the beginning of Step II was not significantly different from run to run.

Downloaded At: 11:17 25 January 2011

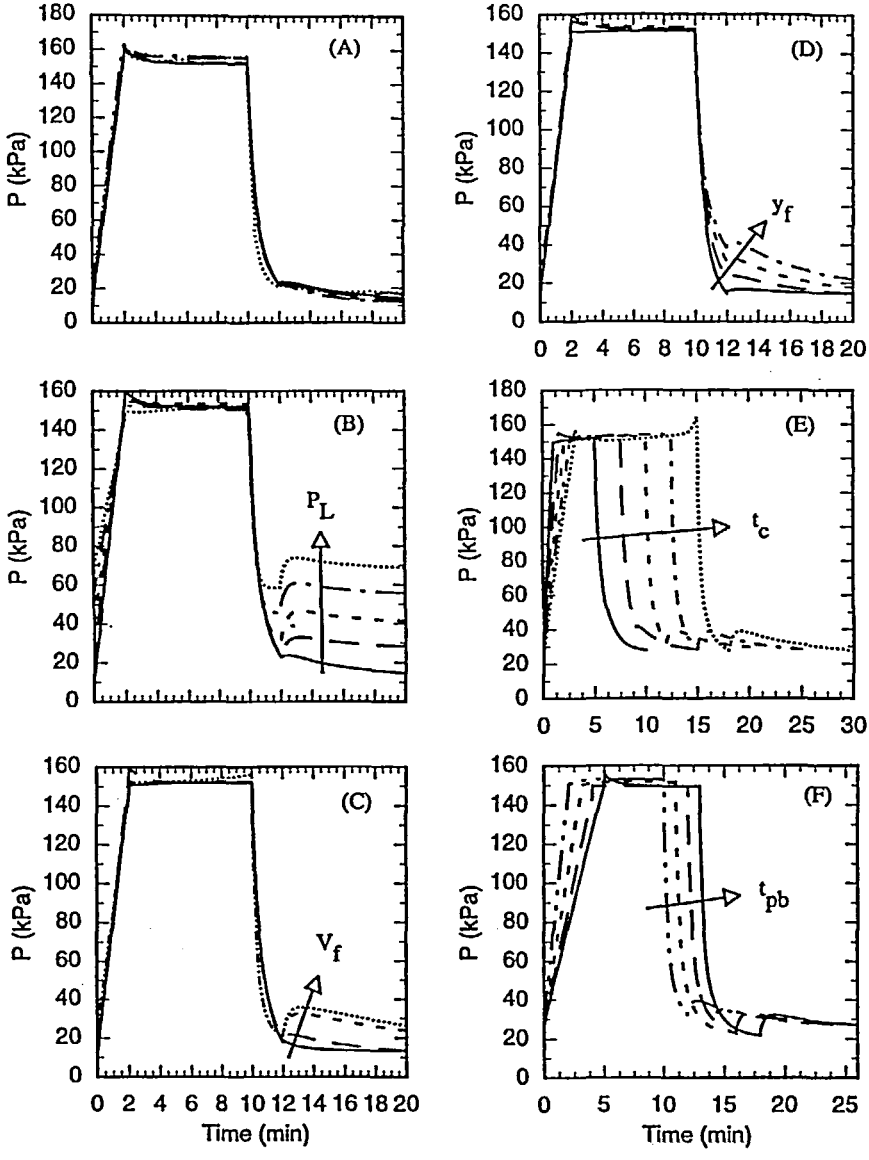

FIG. 2 Pressure histories for all runs, where A to E correspond to the series number in Table 2: (A) γ increases from A1 to A5, almost identical; (B) P_L increases from A1 to B1 to B4; (C) V_f increases from C1 to C4; (D) y_f increases from A1 to D1 to D3; (E) t_c increases from E1 to E5; (F) t_{pb} increases from F1 to F3 to E3.

Downloaded At: 11:17 25 January 2011

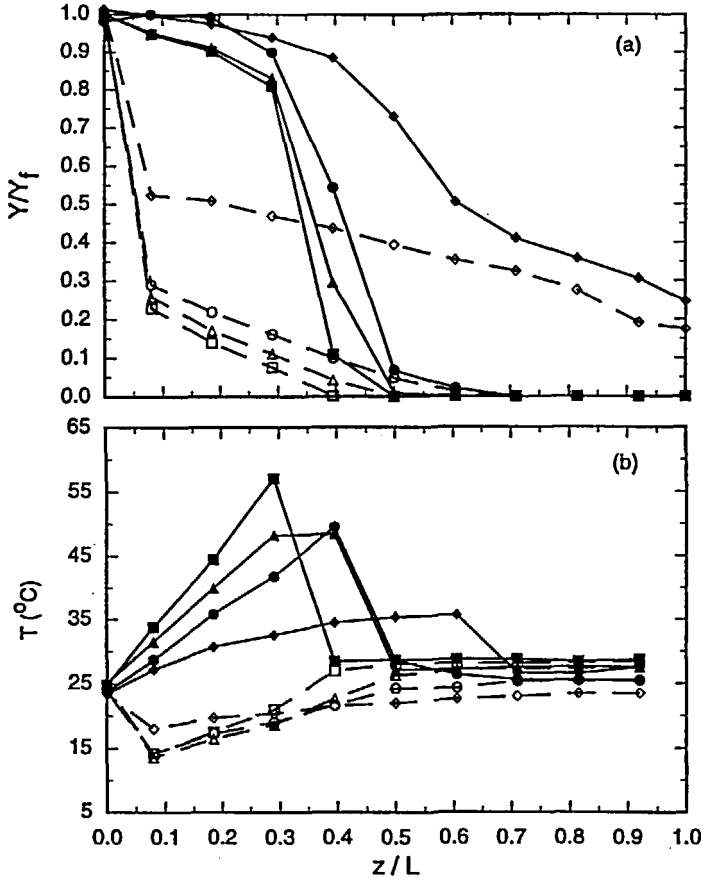

FIG. 3 Butane vapor concentration (a) and temperature (b) profiles at the beginning (empty symbols) and end (solid symbols) of the adsorption step; (■, □) Run A1; (▲, △) Run A3; (●, ○) Run A4; (◆, ◇) Run A5, showing the effect of the purge-to-feed ratio (γ) which decreases with run number.

A decrease in the purge-to-feed ratio corresponded to a decrease in the sweep velocity through the bed, which caused less desorption per cycle and thus a more contaminated bed at the periodic state. The peak temperature decreased with a decrease in the purge-to-feed ratio because as more of the bed became contaminated, the heat of adsorption necessarily decreased on these contaminated portions of the bed, giving rise to smaller increases in the temperatures in these regions. Thus, the periodic state

Downloaded At: 11:17 25 January 2011

temperature swings decreased from about 44 to 18°C with a decrease in the purge-to-feed ratio.

Moreover, when decreasing the purge-to-feed ratio from 1.41 to 0.50, the movement of the concentration wave front was gradual and no butane vapor breakthrough into the light product occurred. However, when decreasing the purge-to-feed ratio from 0.5 to 0.24, an abrupt increase in the contaminated portion of the bed occurred along with breakthrough of butane vapor into the light product. Clearly, a critical purge-to-feed ratio exists for this system ($0.24 < \gamma < 0.5$). However, this critical purge-to-feed ratio may be very difficult to determine a priori because it may depend on the other process conditions. Another unusual feature of these results was that with a volumetric purge-to-feed ratio less than unity, a periodic state was obtained with complete containment of the butane vapor wave front within the bed. This result is in contrast to most of the experimental and theoretical results reported in the literature (3, 5, 15), except for the very recent theoretical work done by Subramanian and Ritter (22). Using equilibrium theory, they showed very clearly that this kind of operation is possible when the effect of velocity variation within the column becomes appreciable. In such circumstances only the process purge-to-feed ratio remains constant (i.e., at the feed and purge inlet conditions), whereas the actual purge-to-feed ratio within the bed varies appreciably because of velocity changes induced by adsorption and desorption, and heating and cooling.

Downloaded At: 11:17 25 January 2011

The process performance indicators for these runs are tabulated in Table 2, graphed in Fig. 4, and summarized in Table 3. The trends were consistent with those reported by Liu and Ritter (17) for the benzene-activated charcoal system, i.e., increasing the purge-to-feed ratio decreased the bed capacity factor and solvent vapor enrichment, whereas it increased the light product purity (i.e., decreased y_P) and solvent vapor recovery. Actually, for all runs with a volumetric purge-to-feed ratio greater than 0.5, the solvent vapor mole fraction in the light product was zero and the butane vapor recovery was 100%. A decreasing bed capacity factor with an increasing purge-to-feed ratio was consistent with the effect of the purge-to-feed ratio on the gas-phase concentration profiles, with a similar explanation. For the smallest purge-to-feed ratio used ($\gamma = 0.24$), the butane vapor enrichment reached as high as 4.2, whereas for the purge-to-feed ratio of 1.41, the butane vapor enrichment was only 2.3. This decrease in the enrichment resulted from the significant dilution effect of increasing the purge-to-feed ratio (17).

Effect of the Purge Pressure

In commercial applications of the PSA–SVR process the adsorption pressure is usually fixed at a pressure slightly higher than atmosphere pressure, leaving

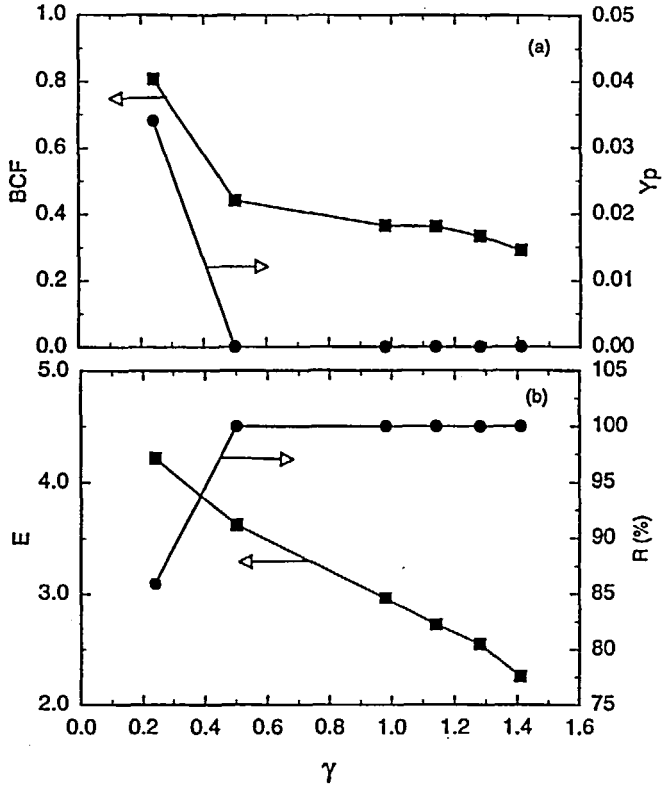

FIG. 4 Effects of the purge-to-feed ratio (γ) on the process performance in terms of the bed capacity factor (BCF), light product purity (y_p), butane vapor enrichment (E), and recovery (R).

the purge pressure as a design parameter. Therefore, it was of interest to investigate the effects of the purge pressure on the process performance. For the effect of the pressure ratio, interested readers are referred to Liu and Ritter (17, 18), and Ritter and Yang (4). Five experiments were carried out to investigate the effect of the purge pressure (Runs A1 and B1 to B4 in Table 2). The magnitude of the purge pressure was varied from 14.7 to 68.8 kPa. The other parameters were fixed, except for the pressure ratio (see Table 2). Since the adsorption pressure was fixed throughout these experiments, the pressure ratio changed with the purge pressure; thus, the results obtained from this series of runs included the combined effects of the purge pressure and pressure ratio. Also, since the purge-to-feed ratio was held constant in all of these runs, the purge gas flow rate was increased when the purge pressure was increased. The pressure histories also varied somewhat from run to run.

Downloaded At: 11:17 25 January 2011

Figure 2(B) displays the pressure histories for these five runs during a periodic cycle. In this series of runs the vacuum level was adjusted so that at the end of the purge step, the column pressure reached the specified purge pressure (P_L). All of the blowdown profiles were nearly identical, except near the end of Step III. The marked differences in this region were caused by changes made in the pressure level of the vacuum surge tank to ensure that the specified purge pressure was reached at the end of Step IV. The sudden increases in pressure that occurred at the beginning of Step IV (that increased with increasing purge pressure) were caused by the successive increases in the purge flow rate with each run. As mentioned above, these purge flow rate increases were required to maintain the volumetric purge-to-feed ratio constant throughout this series of runs. Overall, these differences were considered minor aberrations in the pressure histories, with essentially no effect on the performance.

Downloaded At: 11:17 25 January 2011

The butane vapor concentration and the temperature profiles at the beginning and end of the adsorption step for all five runs are shown in Fig. 5. Increasing the purge pressure moved the butane vapor concentration and bed temperature waves toward the light product end of the bed; however, the changes in these wave fronts were small compared to the effects of some of the other parameters. The differences in the observed maximum temperatures at the end of Step II and the observed minimum temperatures at the beginning of Step II between all five runs were also small. Slight changes in the ambient and feed temperatures between these runs may have caused these differences. The observed maximum (58°C) and minimum (11°C) temperatures also gave rise to periodic state temperature swings of approximately 47°C during these runs, independent of the purge pressure.

The process performance indicators are tabulated in Table 2, graphed in Fig. 6, and summarized in Table 3. For the range of purge pressures investigated, no breakthrough of butane vapor into the light product was observed; therefore, the solvent vapor recovery was 100% and the light product was pure nitrogen for each run. In fact, increasing the purge pressure from 14.7 to 68.8 kPa increased the bed capacity factor only slightly from 0.29 to 0.38. However, the effect of the purge pressure on the solvent vapor enrichment was significant. Increasing the purge pressure from 14.7 to 68.8 kPa decreased the butane vapor enrichment from 2.26 to 1.40, i.e., the average mole fraction of butane vapor flowing out of the bed during the blowdown and purge steps decreased from 45.1 to 27.9%. These trends were consistent with those reported elsewhere (17). There are two plausible explanations for this effect on the enrichment. First, increasing the purge pressure moved the operating point of the purge pressure on the isotherms toward the saturation region of the isotherms; therefore, more butane stayed in the adsorbed phase with increasing purge pressures, which gave rise to less desorption. Second, the

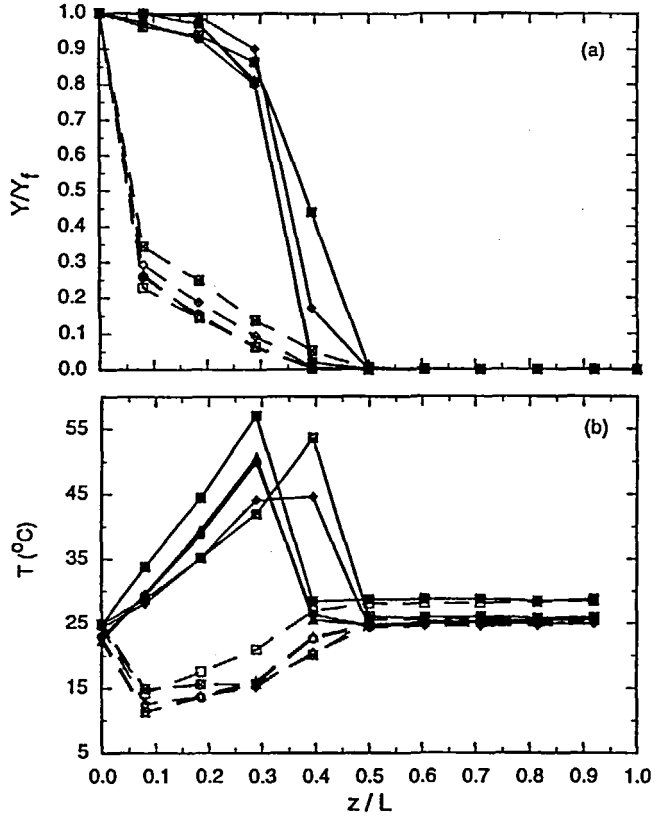

FIG. 5 Butane vapor concentration (a) and temperature (b) profiles at the beginning (empty symbols) and end (solid symbols) of the adsorption step: (■, □) Run 1; (▲, △) Run B1; (●, ○) Run B2; (◆, ◇) Run B3; (⊠, ⊠) Run B4, showing the effect of the purge pressure (P_L) which increases with run letter/number.

constant purge-to-feed ratio requirement resulted in an increase in the purge flow rate each time the purge pressure was increased, which increasingly diluted the purge effluent.

Effect of the Feed Flow Rate

Significant increases or decreases in the volumetric feed flow rate are not unusual in some PSA–SVR operations, especially in large gasoline-tank-filling operations. However, the effect of the feed flow rate on the PSA–SVR process performance has not been studied experimentally. Therefore, four experiments were carried out to investigate its effect (Runs C1 to C4 in Table 2). The magnitude of the feed flow rate was varied from 1.5 to 4.0 SLPM by proportionally

Downloaded At: 11:17 25 January 2011

increasing the nitrogen and butane flow rates (to keep the feed concentration constant). An attempt was made to keep all of the other conditions constant. However, in order to keep the volumetric purge to-feed ratio constant when increasing the volumetric feed flow rate, the purge flow rate was increased. The pressure histories also varied somewhat from run to run.

Figure 2(C) displays the pressure histories for these four runs during a periodic cycle. For the runs operated at the two highest feed flow rates (Runs C3 and C4), sudden increases in the pressure occurred at the beginning of Step IV, and the desired low pressure of 13.8 kPa was not reached at the end of the Step IV. These differences in the pressure histories were caused by the increase in the purge flow rate with each run, coupled with limitations in the size of the exhaust lines and the vacuum pump. As mentioned above, the purge flow rate was increased when the feed flow rate was increased to maintain the purge-to-feed ratio constant throughout this series of runs.

Downloaded At: 11:17 25 January 2011

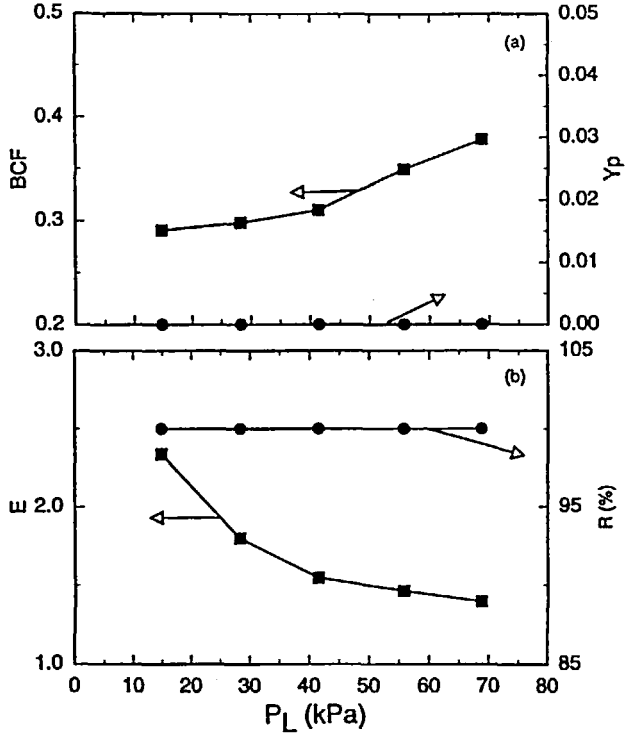

FIG. 6 Effects of the purge pressure (P_L) on the process performance in terms of the bed capacity factor (BCF), light product purity (y_p), butane vapor enrichment (E), and recovery (R).

However, since the purge flow used in these experiments was based on the target values of the purge pressure (13.8 kPa) and since the purge pressure deviated significantly from this target value in the last two runs (~25 kPa), the purge-to-feed ratio changed from 1.50 to 0.83 when changing the volumetric feed flow rate from 2.5 to 3.5 SLPM (see Table 2). So, two of these runs were operated at a high purge-to-feed ratio and the other two at a low purge-to-feed ratio; nevertheless the results were easily interpreted based on results obtained from the purge-to-feed ratio and purge pressure studies.

The butane vapor concentration and the temperature profiles at the beginning and end of the adsorption steps for all four runs are shown in Fig. 7. Increasing the volumetric feed flow rate moved both the concentration and

Downloaded At: 11:17 25 January 2011

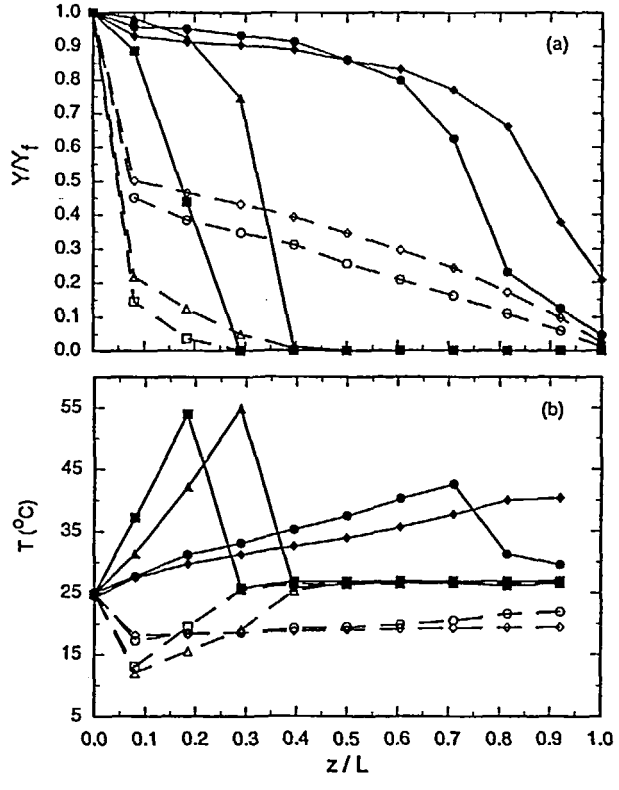

FIG. 7 Butane vapor concentration (a) and temperature (b) profiles at the beginning (empty symbols) and end (solid symbols) of the adsorption step; (■, □) Run C1; (▲, △) Run C2; (●, ○) Run C3; (◆, ◇) Run C4, showing the effect of the volumetric feed flow rate (V_f) which increases with run number.

temperature waves toward the light product end of the bed, mainly because more butane was fed into the bed with an increase in the feed flow rate. However, the corresponding increase in convection with an increase in the feed flow rate may have played a role. At the beginning of the adsorption step the temperatures within the MTZ for all four runs fell below the ambient temperature. In fact, for the two highest feed flow rates at the beginning of Step II, the entire bed was below the ambient temperature and relatively constant at about 17°C. Nevertheless, the observed minimum temperatures for all four runs were similar and ranged between 12 and 17°C. At the end of the adsorption step the observed maximum temperatures for all four runs were significantly above the ambient temperature, but the magnitudes (approximately 55°C) were similar and more pronounced for the two lowest feed flow rates. The observed maximum temperatures for the two runs at the highest feed flow rates were also similar, but they reached only about 40°C. So the periodic state temperature swings ranged from 23°C at the two higher feed flow rates to 43°C at the two lower feed flow rates. This disparity between the temperature swings with an increase in the feed flow rate was understood by referring to the concentration profiles. It was very clear that adsorption was occurring on a less regenerated adsorbent; thus, the amount of butane adsorbed at a specific position during the cycle was less, which necessarily produced less heat and correspondingly smaller temperature rises. Some of the heat may have also been convected out of the bed.

Downloaded At: 11:17 25 January 2011

The large increase in the contaminated portion of the bed that occurred between Runs C2 and C3, corresponding to the feed flow rate increasing from 2.5 to 3.5 SLPM, was most likely caused by the change in the purge-to-feed ratio which was manifested by the change in the purge pressure (as discussed above). Recall that the effect of the purge pressure on the degree of bed contamination (or position of the MTZ) was minimal; however, the effect of the purge-to-feed ratio was marked. This large difference in the position of the MTZ was consistent with a decrease in the purge-to-feed ratio, and since increasing the feed flow rate has the same effect as decreasing the purge-to-feed ratio, the change in purge-to-feed ratio simply enhanced the effect of the feed flow rate. These results showed clearly that the process performance may be very sensitive to minor changes in the purge pressure (see Fig. 2C) because of the effect it has on the purge-to-feed ratio.

The process performance indicators for these runs are tabulated in Table 2, graphed in Fig. 8, and summarized in Table 3. Increasing the feed flow rate increased the bed capacity factor and butane vapor enrichment, but decreased the light product purity (i.e., it increased y_p) and solvent vapor recovery. This was true for both sets of runs; i.e., the effect of the decrease in the purge-to-feed ratio between Runs C2 and C3 did not change these qualitative trends (quantitative effects are discussed below). The reason for the increase

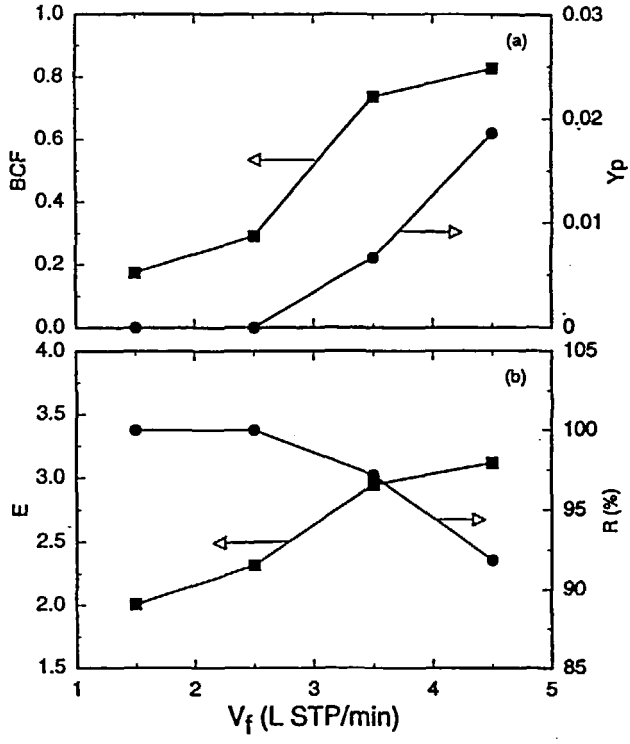

FIG. 8 Effects of the feed volumetric flow rate (V_f) on the process performance in terms of the bed capacity factor (BCF), light product purity (y_p), butane vapor enrichment (E), and recovery (R).

in the bed capacity factor was the same as that given above for the movement of the concentration waves. This increase in the bed capacity factor with the feed flow rate also decreased the amount of unused carbon available for preventing breakthrough of butane into the light product. Thus, eventually breakthrough occurred, which caused the increase in the solvent vapor mole fraction in the light product and decrease in butane vapor recovery. The increase in enrichment with the feed flow rate was unexpected, especially when breakthrough occurred. In fact, the effect of the feed flow rate on butane vapor enrichment for the benzene-activated charcoal system (17, 18) was just the opposite to that observed in this study, where the other trends were the same. Again, the process conditions for these two systems were different, and the system characteristics, such as the adsorption isotherms, were also quite different. All of these differences may have contributed to this intriguing

Downloaded At: 11:17 25 January 2011

discrepancy, but not the incidental changes that occurred in the purge pressure and thus the purge-to-feed ratio.

According to the effects of the purge pressure, a slight increase in it causes a slight decrease in the butane vapor enrichment and has no effect on the bed capacity factor. In contrast, according to the effects of the purge-to-feed ratio, a significant decrease in it causes a large increase in both the bed capacity factor and enrichment. So the effects of the purge pressure were most likely overwhelmed by the effects of the purge-to-feed ratio; and again, since increasing the feed flow rate has the same effect as decreasing the purge-to-feed ratio, the change in the purge-to-feed ratio simply enhanced the effect of the volumetric feed flow rate (see Fig. 8).

Effect of the Feed Concentration

A PSA–SVR process must be designed to handle the highest feed concentration expected, and similarly to the feed flow rate, large variations are anticipated. An experimental investigation of the effect of feed concentration on the PSA–SVR process was carried out by Ritter and Yang (3), but only with an emphasis on the light product purity. Therefore, four experiments were carried out to investigate the effect of the feed concentration (y_f) (Runs A1 and D1 to D3 in Table 2). The magnitude of feed mole fraction was varied from 9.5 to 39.3 vol% butane in nitrogen. An attempt was made to keep all of the other parameters constant, but the pressure histories varied somewhat from run to run.

Downloaded At: 11:17 25 January 2011

Figure 2(D) displays the pressure histories for these runs during a periodic cycle. All of the blowdown profiles were similar, except near the end of Step III. A similar problem occurred here as in the feed flow rate study. Because of the increasing amount of butane vapor desorbing during the blowdown step with increasing feed concentration, the pressure at the end of both the blowdown and purge steps increased consistently with increasing feed mole fraction; and for the last two runs, the desired purge pressure of 14.7 kPa was not reached even at the end of Step IV (see Table 2). Nevertheless, similar low pressures were reached in Runs D2 and D3, which caused reasonably similar changes in the purge-to-feed ratio from about 1.4 to 1.0. So two of these runs were operated essentially at a high purge-to-feed ratio and the other two at a low purge-to-feed ratio. Thus, the trends were easily interpreted based on results obtained from the purge pressure and purge-to-feed ratio studies.

The butane vapor concentration and temperature profiles at the beginning and end of the adsorption steps for all four runs are shown in Fig. 9. Increasing the feed mole fraction moved the concentration and temperature waves toward the light product end of the bed. However, in this set of runs the observed peak temperatures at the end of the adsorption step exhibited a maximum with increasing feed mole fraction (66°C for $y_p = 31.4\%$). The increase in temperature with an increase in the feed mole fraction was easily understood

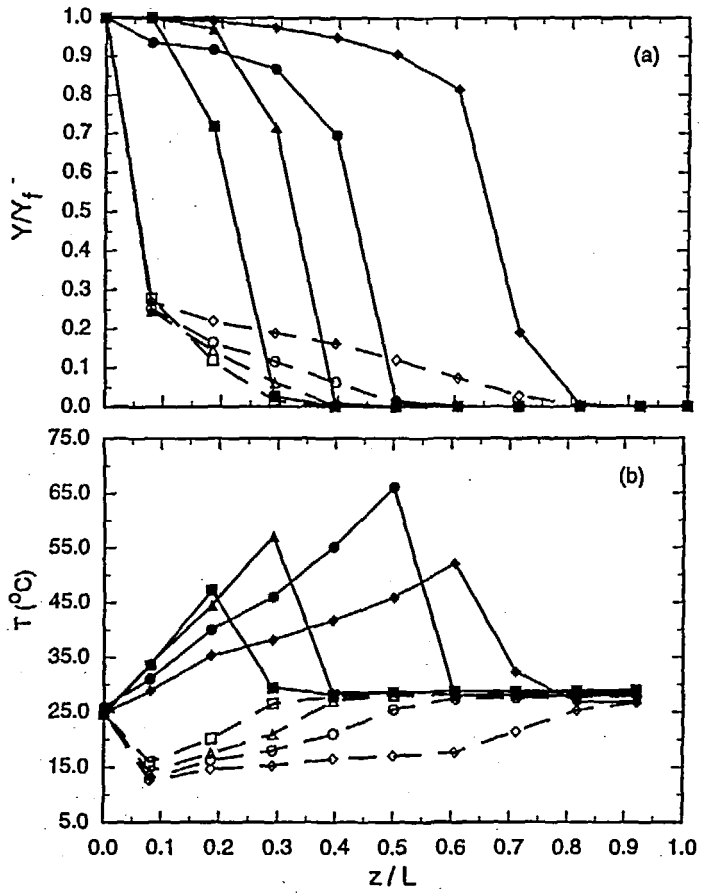

FIG. 9 Butane vapor concentration (a) and temperature (b) profiles at the beginning (empty symbols) and end (solid symbols) of the adsorption step; (■, □) Run D1; (▲, △) Run A1; (●, ○) Run D2; (◆, ◇) Run D3, showing the effect of the feed concentration (y_f) which increases in the order presented from D1 to D3.

and related to the increase in the number of moles of butane vapor being fed into the bed per cycle. The observed maximum in the temperature may have been caused by the increase in the contaminated portion of the bed, which occurred with a corresponding increase in the MTZ. These two changes increased the region over which the heat of adsorption was distributed. Also, since the temperature wave fronts moved toward the light product end of the bed with increasing feed mole fraction (y_f), some of the heat may have been

Downloaded At: 11:17 25 January 2011

convected out of the bed. The periodic state temperature swings also went through a maximum ranging between 40 and 54°C; and as the feed mole fraction increased, more of the bed exhibited below ambient temperatures at the beginning of Step II due to desorption cooling occurring over a larger region of the bed. It was doubtful that the changes in purge pressure and purge-to-feed ratio caused the observed maximum in the peak temperature because it occurred between Runs D2 and D3, and a lower purge-to-feed ratio causes a higher temperature swing (see Fig. 3).

The process performance indicators are tabulated in Table 2, graphed in Fig. 10, and summarized in Table 3. For all four feed concentrations there was no breakthrough of butane vapor into the light product; therefore, the recovery of butane vapor was 100% and the butane vapor concentration in

Downloaded At: 11:17 25 January 2011

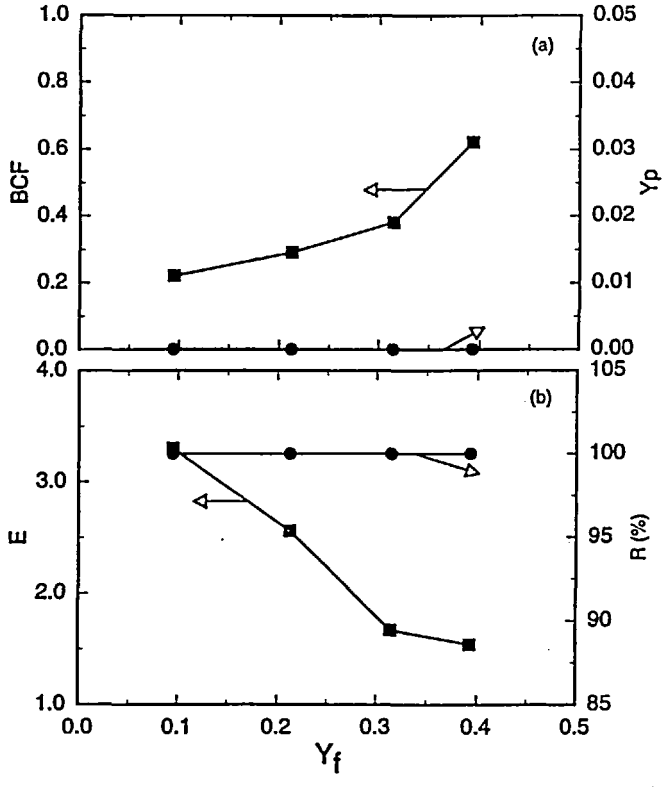

FIG. 10 Effects of the feed concentration (y_f) on the process performance in terms of the bed capacity factor (BCF), light product purity (y_p), butane vapor enrichment (E), and recovery (R).

the light product was zero. Nevertheless, the increase in the bed capacity factor with increasing feed mole fraction was significant, e.g., it increased from 0.22 to 0.62 with the feed mole fraction increasing from 9.5 to 39.3 vol%. The butane vapor enrichment also exhibited a marked decrease from 3.30 to 1.54 over the same change in the feed mole fraction. These trends were consistent with those reported elsewhere (17). The increase in the bed capacity factor with increasing feed mole fraction was easily understood and explained above in terms of the increase in temperature. Also, the lower purge-to-feed ratio used in Runs D2 and D3 most likely enhanced this increase in the BCF because the effects of increasing the feed concentration and decreasing the purge-to-feed ratio on the bed capacity factor were complementary. The explanation for the decrease in the solvent vapor enrichment with increasing feed concentration was not so obvious. It may have been caused by the higher partial pressure of butane vapor during the blowdown and purge steps for the runs with higher feed mole fraction; thus, relatively less desorption occurred at a specific position in the bed. Also, the slight increase in the purge pressure that occurred for Runs D2 and D3 may have augmented the effect of the feed concentration on the enrichment since the effect of the purge pressure on the enrichment was the same. Moreover, the effect of changing the purge-to-feed ratio for Runs D2 and D3 probably dampened the effect of the feed concentration on the enrichment because the effect of the purge-to-feed ratio on the solvent vapor enrichment was the opposite.

Downloaded At: 11:17 25 January 2011

Effect of the Cycle Time

The cycle time is one of the more important design variables in PSA processes, as it sets the column size. Clearly, if the cycle time is too long, breakthrough occurs, and if it is too short, the adsorbent is underutilized. Nevertheless, very few studies have investigated the effect of the cycle time on process performance. Therefore, five experiments were performed to investigate its effect (Runs E1 to E5 in Table 2). The magnitude of the cycle time was varied from 10 to 30 minutes, where the step times were scaled in proportion to the cycle time. For example, when the cycle time was decreased from 20 to 10 minutes, the equal feed and purge times of 8 minutes and the equal pressurization and blowdown times of 2 minutes were decreased to 4 and 1 minutes, respectively. All of the other parameters were fixed. A higher feed mole fraction and a lower purge-to-feed ratio were used in these five runs compared to all of the previous runs to cover the conditions with and without breakthrough of butane vapor into the light product. Also, anticipating problems at this high feed concentration, a higher purge pressure was used for all five runs to ensure that the desired purge pressure at the end of Step IV was reached. The pressure histories also varied slightly from run to run.

Figure 2(E) displays the pressure histories for these five runs during a periodic cycle. The only major differences in the pressure histories occurred at the beginning of Step IV where sudden increases in the pressure were

exhibited for the three longest cycle times (Runs E3, E4, and E5). These sudden increases were caused by the onset of the purge flow, coupled with the increased amount of butane vapor entering the column with increasing cycle time and the limitations in the size of the exhaust lines and the vacuum pump. A similar discrepancy between the pressure histories occurred in the feed flow rate study; however, in this case, at the end of Step IV, the desired purge pressure of 27.6 kPa was reached in nearly all runs. So the purge-to-feed ratio was not affected significantly over the purge step duration, and thus the effect of these minor variations in the pressure histories between the shorter and longer cycle times was considered negligible.

The butane vapor concentration and the temperature profiles at the beginning and end of the adsorption step for all five runs are shown in Fig. 11.

Downloaded At: 11:17 25 January 2011

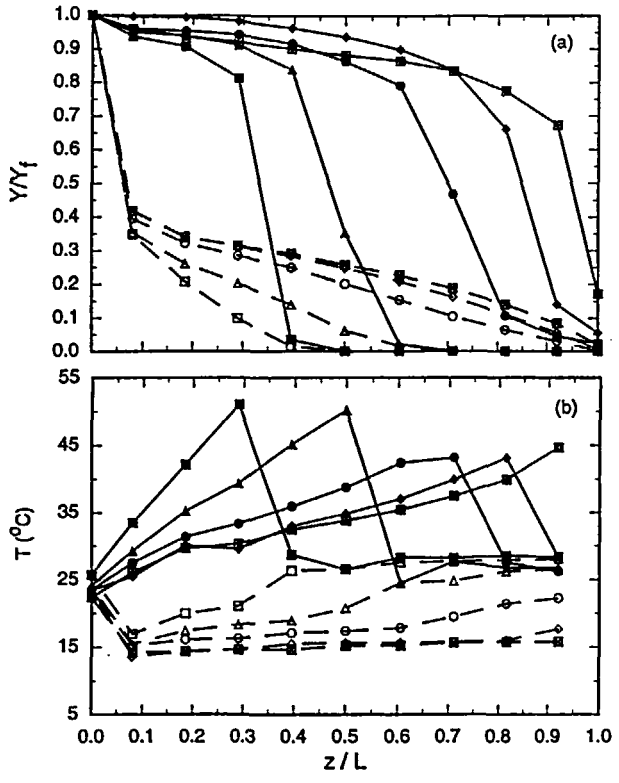

FIG. 11 Butane vapor concentration (a) and temperature (b) profiles at the beginning (empty symbols) and end (solid symbols) of the adsorption step; (■, □) Run E1; (▲, △) Run E2; (●, ○) Run E3; (◆, ◇) Run E4; (⊠, ☒) Run E5, showing the effect of the cycle time (t_c) which increases with run number.

Increasing the cycle time increased the amount of butane vapor fed into the bed during a cycle, which necessarily moved the concentration and temperature wave fronts toward the light product end of the bed. Moreover, for the process conditions used in this series of experiments, butane vapor breakthrough into the light product occurred for cycle times greater than or equal to 20 minutes, and a significant jump in the concentration profile occurred when increasing the cycle time from 15 to 20 minutes. This unusual behavior was also manifested in the temperature profiles which exhibited two different maxima depending on whether breakthrough occurred or not. For cycle times of 10 and 15 minutes the observed maximum temperature was about 52°C, whereas for cycle times of 20, 25, and 30 minutes it was about 44°C. However, the effect of the cycle time on the periodic state temperature swings was minimal, with swings ranging between 30 and 35°C; the smaller temperature swings corresponded to the longer cycle times. Also, for the two longest cycle times, at the beginning of Step II, the entire bed was below the ambient temperature and relatively constant at about 15°C. More marked but similar trends were observed in the feed flow rate study, and for similar reasons. It was very clear that adsorption was occurring on a less regenerated adsorbent; thus, the amount of butane adsorbed at a specific position during the cycle was less, which necessarily produced less heat and correspondingly smaller temperature rises. Some of the heat may have also been convected out of the bed, however.

Downloaded At: 11:17 25 January 2011

The process performance indicators are tabulated in Table 2, graphed in Fig. 12, and summarized in Table 3. Increasing the cycle time from 10 to 30 minutes increased the bed capacity factor from 0.32 to 0.82, with breakthrough occurring at a bed capacity factor of 0.73. Once breakthrough occurred, the light product mole fraction increased and the butane vapor recovery decreased with increasing cycle time. The butane vapor enrichment, on the other hand, exhibited a maximum with increasing cycle time, similar to that shown by Liu and Ritter for the benzene-activated charcoal system (17). In both cases the maximum in butane vapor enrichment corresponded to the cycle time at which significant amounts of solvent vapor began breaking through the bed during the adsorption step. The decrease in butane vapor enrichment with increasing cycle time (after breakthrough) was easily understood and verified in both rigorous and ideal modeling studies (15, 17). It was caused by the loss of the solvent vapor into the light product. However, the increase in enrichment with increasing cycle time (before breakthrough) was not so easily understood. The ideal modeling study (15) predicted no effect, whereas the rigorous modeling study (17) agreed with these experimental findings. So the cause had to be related to one or more of the many nonidealities included in the rigorous modeling study, and necessarily included in the experimental results.

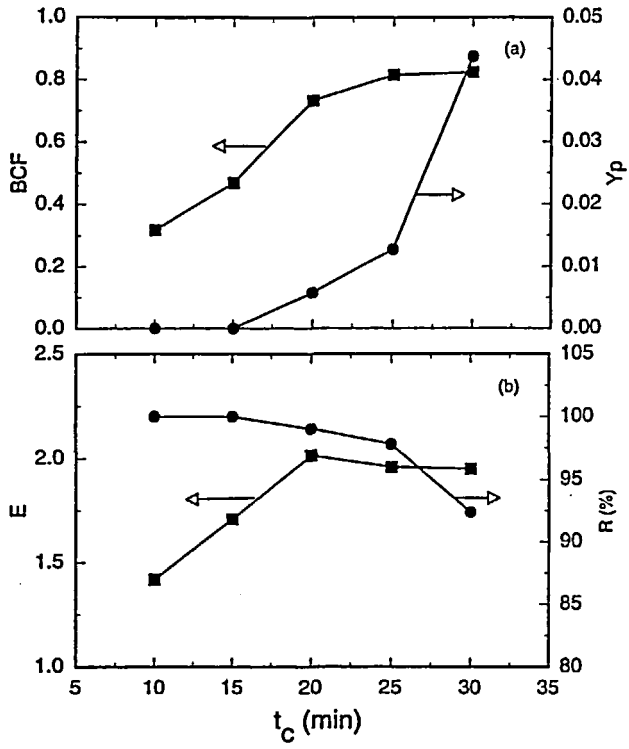

FIG. 12 Effects of the cycle time (t_c) on the process performance in terms of the bed capacity factor (BCF), light product purity (y_p), butane vapor enrichment (E), and recovery (R).

Downloaded At: 11:17 25 January 2011

It was also intriguing that the bed capacity factor was only 0.73 when slight breakthrough occurred. Similar results were observed in the feed flow rate, cycle time, and pressurization/blowdown step time studies. Under the most ideal conditions, i.e., isothermal, equilibrium, negligible dispersion, etc., the width of the MTZ at the end of Step II is infinitesimally small (corresponding to a shock wave profile) and breakthrough occurs at a bed capacity factor of unity (14, 15). Thus, the bed capacity factor at which breakthrough occurs may be used to judge how much the process deviates from the most ideal conditions. In this PSA process, significant deviations from ideality occurred, where all of the nonidealities (lumped together) played a significant role in controlling the shape of the MTZ, which was quite broad.

Effect of the Pressurization and Blowdown Times

The dynamics of the pressurization and blowdown steps in a PSA process have been investigated by several researchers (23–25). However, none of

these studies have reported the effects of the pressurization/blowdown step time (t_{pb}) on the PSA process performance. Yet, in some PSA systems, especially PSA–SVR, this parameter dictates the size of the vacuum system. Therefore, it was of interest to investigate the effects of the pressurization/blowdown step time on the process performance. Four experiments were performed to investigate this effect (Runs F1 to F3, and E3 in Table 2). The magnitude of the pressurization/blowdown step time was varied from 2 to 5 minutes with the adsorption/purge step time fixed at 8 minutes. In these runs the cycle time ranged from 20 to 26 minutes, which also changed the throughput (τ), defined as the volume of feed processed per time per mass of adsorbent (17). Clearly, as the pressurization/blowdown step time increased, the throughput decreased. All of the other parameters were fixed. A higher feed mole fraction and purge pressure, as well as a lower purge-to-feed ratio, were used in these four runs to be consistent with the cycle time study. The pressure histories were also fairly consistent from run to run.

Figure 2(F) displays the pressure histories for these runs during a periodic cycle. All of these blowdown profiles were nearly identical, except near the end of Step III. In this region the profiles differed slightly because the time for blowdown increased with increasing pressurization/blowdown step time. In fact, as the pressurization/blowdown step time increased, the pressure at the end of Step III decreased slightly and actual fell below the desired purge pressure. At the beginning of Step IV, however, the (familiar) sudden increases in pressure occurred for all runs, and the desired purge pressure was reached by the end of Step IV. So, these pressure histories were sufficiently similar to reveal the effect of pressurization/blowdown step time without being obscured by the slight changes observed from run to run.

The butane vapor concentration and temperature profiles at the beginning and end of the adsorption step for all four runs are shown in Fig. 13. The butane vapor concentration and temperature profiles did not vary significantly with variation in the pressurization/blowdown step time, although slight trends were observed. For example, decreasing the pressurization/blowdown step time moved the concentration wave front toward the light product end of the bed. However, the slight changes in the temperature profiles may have been caused by the slight differences in the ambient and feed temperatures of these runs, which may have also affected the concentration profiles. The observed maximum (45°C) and minimum (13°C) temperatures in the bed during these runs gave rise to rather small periodic state temperature swings of approximately 32°C. These relatively small temperature swings were consistent with those observed in some of the other parametric studies (e.g., the purge-to-feed ratio, cycle time, and feed flow rate) when breakthrough of butane into the light product occurred. Breakthrough was exhibited by all of the runs in this series, indicating that a considerable portion of the bed was

Downloaded At: 11:17 25 January 2011

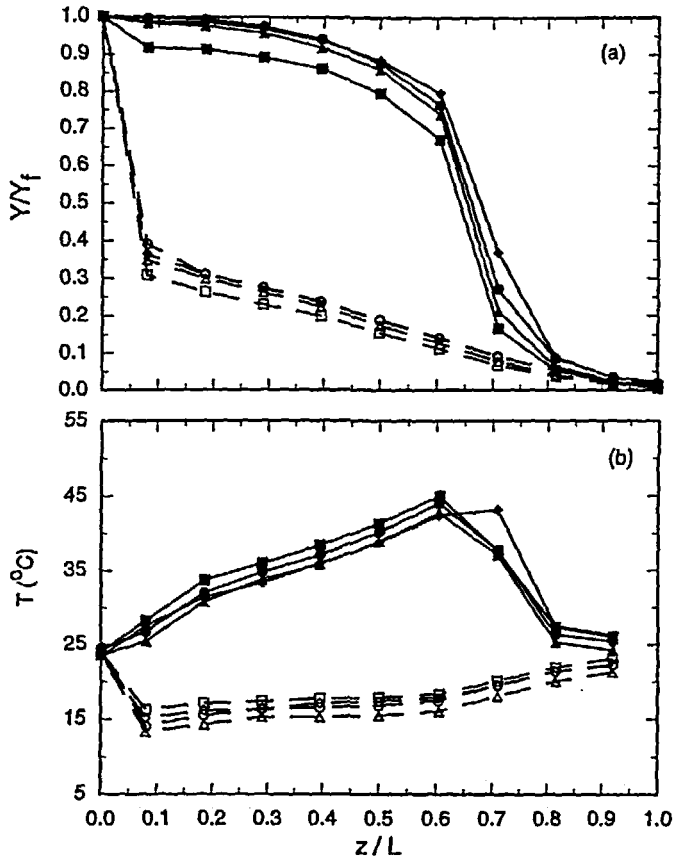

FIG. 13 Butane vapor concentration (a) and temperature (b) profiles at the beginning (empty symbols) and end (solid symbols) of the adsorption step: (■, □) Run F1; (▲, △) Run F2; (●, ○) Run F3; (◆, ◇) Run E3, showing the effect of the pressurization and purge step time (t_{pb}) which decreases in the order presented from F1 to E3.

contaminated, which may have allowed the heat to be more easily distributed within and convected from the bed.

The process performance indicators are tabulated in Table 2, graphed in Fig. 14, and summarized in Table 3. Increasing the pressurization/blowdown step time from 2 to 5 minutes degraded the process performance because the bed capacity factor and the solvent vapor mole fraction in the light product both increased slightly and the butane vapor recovery decreased. On the other hand, the butane vapor enrichment remained relatively constant with increas-

Downloaded At: 11:17 25 January 2011

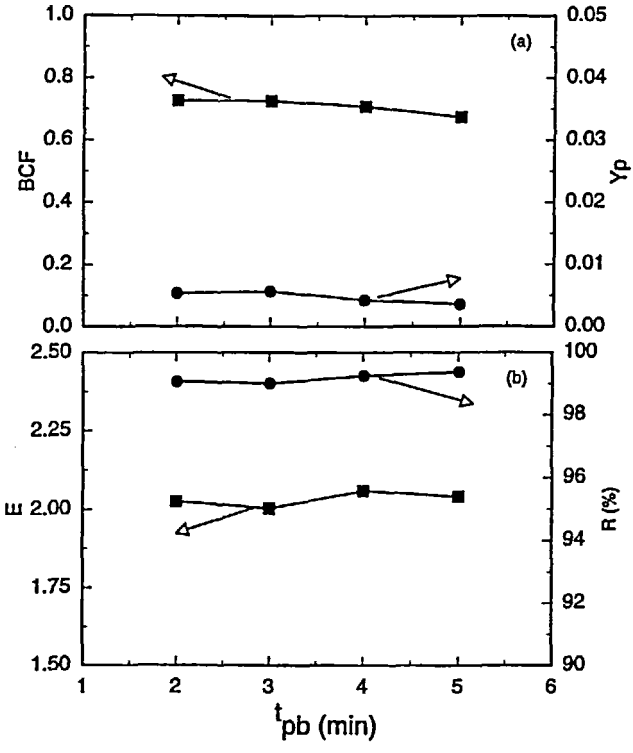

FIG. 14 Effects of the pressurization and blowdown step time (t_{pb}) on the process performance in terms of the bed capacity factor (BCF), light product purity (y_p), butane vapor enrichment (E), and recovery (R).

ing the pressurization/blowdown step time. Therefore, in terms of these parameters, the effects of the pressurization/blowdown step time on the process performance were negligible, but not in terms of some other measures.

Table 4 lists the time-average mole fractions and percentage recoveries of the butane vapor during the blowdown and purge steps at the periodic state for four out of the six series of runs. Considering the short blowdown step time compared to the purge step time, the percentage recoveries achieved during blowdown were quite high for most of the runs. Moreover, the mole fractions of the butane vapor during blowdown were also quite high. Generally, the average mole fraction during the blowdown and purge steps increased with an increase in the bed capacity factor, and so did the percentage recovery during the purge step, unless significant breakthrough occurred (compare R_{IV} of Run A5 with those of Runs A1 to A4, Run C4 with those of Runs C1 to

Downloaded At: 11:17 25 January 2011

C3, and Run E5 with those of Runs E1 to E4). However, the percentage recovery during blowdown decreased with an increase in the bed capacity factor. This last trend may have been related to the volumetric flow rate (at STP) being small when the effluent concentration was high during the blowdown step, possibly due to readsorption occurring in less saturated regions in the bed.

Nevertheless, the average mole fraction increased quickly with an increase in the blowdown step time (E and F series), especially when the feed step time was fixed. For example, when the 8-minute feed step time was used (Runs F1, F2, and F3), the average mole fraction during the blowdown step reached as high as 86.9% for the 5-minute blowdown and purge cycle (Run F1). Clearly, a longer blowdown step allowed more time for the carrier gas to leave the bed, which in turn allowed more time for butane to desorb and leave the bed essentially undiluted. The effluent concentration histories displayed in Fig. 9(f) of Part I (21) show this trend very clearly. This result provides some valuable insight into constructing new PSA–SVR cycle configurations to improve the solvent vapor enrichment, i.e., the blowdown time can be increased and the purge time decreased to increase the solvent vapor

Downloaded At: 11:17 25 January 2011

TABLE 4
PSA–SVR Periodic Bed Capacity Factors, Time-Averaged Mole Fractions, and Percent Recoveries of Butane during the Blowdown and Purge Steps

Run	y_f (%)	BCF (—)	y_{III} (%)	y_{IV} (%)	R_{III} (%)	R_{IV} (%)
A1	21.2	0.29	49.2	47.5	41.1	58.9
A2	20.8	0.33	49.9	53.9	38.7	61.3
A3	21.8	0.36	53.0	61.0	39.6	60.4
A4	20.4	0.44	50.2	63.0	37.9	62.1
A5	20.8	0.81	54.5	80.5	35.6	51.2
C1	19.7	0.17	35.3	40.6	54.6	45.4
C2	20.9	0.30	50.6	47.9	40.2	59.8
C3	20.6	0.74	70.0	58.3	26.3	71.2
C4	20.6	0.83	70.0	62.8	22.9	70.5
E1	34.0	0.32	46.9	48.6	41.5	58.5
E2	34.9	0.47	62.5	59.3	39.0	61.0
E3	35.8	0.73	78.4	70.5	32.3	66.6
E4	35.3	0.81	78.0	67.1	30.1	67.7
E5	35.6	0.82	73.3	68.4	28.5	65.1
F1	34.5	0.67	86.9	59.5	48.2	51.2
F2	34.9	0.71	86.9	64.2	47.0	52.5
F3	34.4	0.73	82.9	67.1	41.4	57.7

enrichment by minimizing the diluting effects of purge. However, the expense of this increased enrichment is a larger bed capacity factor, which suggests that the throughput may suffer.

CONCLUSIONS

A unique PSA–SVR system was used to investigate the periodic process performance of butane vapor recovery from nitrogen using Westvaco BAX activated carbon. The effects of six important process and operating parameters were investigated, i.e., the purge-to-feed ratio, purge pressure, volumetric feed flow rate, feed concentration, cycle time, and pressurization/blowdown step time. General observations are given below, followed by specific trends. These observations and trends should give some useful insight into the design of more efficient PSA–SVR processes.

Downloaded At: 11:17 25 January 2011

The temperature swings associated with changes in all of these parameters were very similar, ranging from a maximum of 54°C when changing the feed mole fraction to a minimum of 18°C when changing the purge-to-feed ratio. Also, the temperature swings decreased as the bed became more contaminated, especially when breakthrough occurred, which led to the supposition that heat was being distributed more evenly within and also convected from the bed. These results demonstrated the importance of accounting for heat effects in PSA–SVR systems. As the bed became more contaminated, the MTZ also increased, indicating the system was becoming more nonideal. Finally, the effects of most of these parameters on the process performance were consistent with simulation results in the literature; however, some opposite trends were observed.

Increasing the purge-to-feed ratio improved the process performance (except for decreasing the solvent vapor enrichment) because the solvent vapor recovery increased and the bed capacity factor and the light product mole fraction decreased. Moreover, periodic states were obtained without butane vapor breaking through into the light product for volumetric purge-to-feed ratios of 0.98 and 0.50 but not for 0.24. These results verified for the first time that the concentration wave can be contained within the bed at the periodic state, even with a volumetric purge-to-feed ratio less than unity, because of local velocity variation manifested by adsorption and heat effects. This result also indicated that a critical volumetric purge-to-feed ratio exists ($0.24 < \gamma < 0.5$), but this critical purge-to-feed ratio may be difficult to determine because it may depend on the other process conditions. Surprisingly, the purge pressure had only a small effect on the bed capacity factor, but it had a large effect on the butane vapor enrichment which decreased with increasing purge pressure. The experimental results also revealed that the process performance may be very sensitive to minor changes in the purge pressure because of the

effect it has on the purge-to-feed ratio. Increasing the volumetric feed flow rate worsened the process performance because the butane vapor recovery decreased and the bed capacity factor and light product mole fraction increased. However, increasing the volumetric feed flow rate increased the butane vapor enrichment, which was opposite to that reported in the literature. This result provided evidence for the many subtle differences that may exist between the performance of seemingly similar PSA–SVR processes. Increasing the feed concentration deteriorated the process performance because the bed capacity factor increased and the butane vapor enrichment decreased. In contrast, increasing the cycle time decreased the butane vapor recovery and increased the bed capacity factor and light product mole fraction; however, it caused the butane vapor enrichment to go through a maximum, which corresponded to the onset of butane vapor breakthrough. All of these trends were consistent with results reported in the literature. The effect of the pressurization/blowdown step time on the average mole fraction and recovery of the partitioned effluents during the blowdown and purge steps provided valuable insight into new PSA–SVR cycle configurations that may increase the solvent vapor enrichment.

Downloaded At: 11:17 25 January 2011

NOMENCLATURE

A	adsorption isotherm parameter (K)
B	adsorption isotherm parameter (K)
b, b_0	adsorption isotherm parameters (kPa^{-1})
E	enrichment
L	bed length (m)
P	pressure (kPa)
q	amount adsorbed (mol/kg)
q_m, q_0	adsorption isotherm parameters (mol/kg)
q^*	equilibrium amount adsorbed (mol/kg)
T	temperature (K)
t_c	cycle time (min)
V	volumetric flow rate (m^3/s)
y	gas phase mole fraction
z	axial position (m)

Greek Symbols

γ	purge-to-feed ratio

Subscripts

cal	calculated

exp	experimental
f	feed
H	high
i	index
L	low
pb	pressurization and blowdown
p	light product
z	axial position
I, II, III, IV	step numbers

ACKNOWLEDGMENT

The authors gratefully acknowledge financial support from the National Science Foundation under Grant CTS-9410630, and from the Westvaco Charleston Research Center.

Downloaded At: 11:17 25 January 2011

REFERENCES

1. D. J. Pezolt, S. J. Collick, H. A. Johason, and L. A. Robbins, "Pressure Swing Adsorption for VOC Recovery at Gasoline Loading Terminals," *Environ. Prog.*, *16*(1), 16–19 (1997).
2. R. J. Holman and J. H. Hill, *New Developments in Hydrocarbon Vapor Recovery*, Paper Presented at AIChE 1992 Annual Meeting, Miami Beach, FL, November 1–6, 1992.
3. J. A. Ritter and R. T. Yang, "Pressure Swing Adsorption: Experimental and Theoretical Study on Air Purification and Vapor Recovery," *Ind. Eng. Chem. Res.*, *30*, 1023–1032 (1991).
4. J. A. Ritter and R. T. Yang, "Air Purification and Vapor Recovery by Pressure Swing Adsorption: A Comparison of Silicalite and Activated Carbon," *Chem. Eng. Commun.*, *108*, 289–305 (1991).
5. E. S., Kikkinides, J. A. Ritter, and R. T. Yang, "Pressure Swing Adsorption for Simultaneous Purification and Sorbate Recovery," *J. Chin. Inst. Chem. Eng.*, *22*, 399 (1991).
6. E. S. Kikkinides and R. T. Yang, "Simultaneous SO_2/NO_x Recovery from Flue Gas by Pressure Swing Adsorption," *Ind. Eng. Chem. Res.*, *30*, 1981–1989 (1991).
7. E. S. Kikkinides, R. T. Yang, and S. H. Cho, "Concentration and Recovery of CO_2 from Flue Gas by Pressure Swing Adsorption," *Ibid.*, *32*, 2714–2720 (1993).
8. K. T. Chue, J. N. Kim, Y. J. Yoo, S. H. Cho, and R. T. Yang, "Comparison of Activated Carbon and Zeolite 13X for CO_2 Recovery from Flue Gas by Pressure Swing Adsorption," *Ibid.*, *34*, 591–598 (1995).
9. E. S. Kikkinides, V. I. Sikavitsas, and R. T. Yang, "Natural Gas Desulfurization by Adsorption: Feasibility and Multiplicity of Cyclic Steady States," *Ibid.*, *34*, 255–262 (1995).
10. J. Izumi, T. Morimoto, and H. Tsutaya, "Sulfur Dioxide Removal and Recovery with Pressure Swing Adsorption form Process Offgas," *AIChE 1992 Annual Meeting Preprint*, pp. 419–422, Miami Beach, FL, November, 2–6, 1992.

11. A. Sasaki, S. Matsumoto, M. Fujitsuka, T. Tanaka, and J. Ohtsuki, "CO_2 Recovery in Molten Carbonate Fuel Cell System by Pressure Swing Adsorption," *IEEE Trans. Energy Conv.*, *8*(1), 26–32 (1993).
12. D. M. Ruthven and S. Farooq, "Concentration of a Trace Component by Pressure Swing Adsorption," *Chem. Eng. Sci.*, *49*, 51–60 (1994).
13. S. Suh and P. C. Wankat, "A New Pressure Swing Adsorption Process for High Enrichment and Recovery," *Ibid.*, *44*, 567–574 (1989).
14. M. D. LeVan, "Pressure Swing Adsorption: Equilibrium Theory for Purification and Enrichment," *Ind. Eng. Chem. Res.*, *34*, 2655–2660 (1995).
15. D. Subramanian and J. A. Ritter, "Equilibrium Theory for Solvent Vapor Recovery by Pressure Swing Adsorption: Analytical Solution for Process Performance," *Chem. Eng. Sci.*, *52*, 3161–3172 (1997).
16. Y. Liu and J. A. Ritter, "Evaluation of Model Approximations in Simulating Pressure Swing Adsorption–Solvent Vapor Recovery," *Ind. Eng. Chem. Res.*, *36*, 1767–1778 (1997).
17. Y. Liu and J. A. Ritter, "Pressure Swing Adsorption–Solvent Vapor Recovery: Process Dynamics and Parametric Study," *Ibid.*, *35*, 2299–2312 (1996).
18. Y. Liu and J. A. Ritter, "Fractional Factorial Study of a Pressure Swing Adsorption–Solvent Vapor Recovery Process," *Adsorption*, *3*, 151–163 (1997).
19. Y. Liu and J. A. Ritter, "Periodic State Heat Effects in Pressure Swing Adsorption–Solvent Vapor Recovery," *Ibid.*, *4*, 159–172 (1998).
20. E. D. Tolles, Westvaco Charleston Research Center, Charleston, SC, personal communication, 1996.
21. Y. Liu, C. E. Holland, and J. A. Ritter, "Solvent Vapor Recovery by Pressure Swing Adsorption. I. Experimental Transient and Periodic Dynamics of the Butane-Activated Carbon System," *Sep. Sci. Technol.*, *33*, 2311–2334 (1998).
22. D. Subramanian and J. A. Ritter, "Equilibrium Theory for Solvent Vapor Recovery by Pressure Swing Adsorption: Analytic Solution for Process Performance with Velocity Variation and Gas Phase Capacitance," *Ibid.*, In Press.
23. R. Schollner, M. Wolf, and G. Kluge, "Experimental and Theoretical Investigations of the Blowdown Step of a PSA Process for H_2-Purification," in *Separation Technology* (E. F. Vansant, Ed.), Elsevier, New York, NY, 1994, pp. 477–487.
24. B. D. Crittenden, J. Guan, W. N. Ng, and W. J. Thomas, "Dynamics of Pressurization and Depressurization during Pressure Swing Adsorption," *Chem. Eng. Sci.*, *49*, 2657–2669 (1994).
25. B. D. Crittenden, J. Guan, W. N. Ng, and W. J. Thomas, "Pressure, Concentration and Temperature Profiles in a 5A Zeolite Adsorbent Bed during Pressurization and Depressurization with Air," *Ibid.*, *50*, 1417–1428 (1995).

Received by editor September 2, 1997
Revision received April 1998

Downloaded At: 11:17 25 January 2011